Radioactive Decay and Associated Electrical Changes in Fast-Neutron-Irradiated CdS†

R. T. JOHNSON, JR., AND B. T. KENNA
Sandia Laboratories, Albuquerque, New Mexico 87115
(Received 6 January 1969; revised manuscript received 19 March 1969)

Changes in resistivity (or conductivity) with time after fast-neutron irradiation have been correlated with the measured decay of radioactivity from CdS. After accounting for effects associated with thermal annealing, the results have shown that induced conductivity results from the β decays of ^{115}Cd (2.3-day half-life) and ^{32}P (14.3-day half-life). Ionization resulting from the absorption of β radiation produces the induced conductivity. Absorption of γ radiation from the ^{115}Cd decay was insignificant. The electron free lifetime τ_n was determined from the induced conductivity, the mobility, the β-decay rate, the radiation-ionization energy, and the average energy absorbed per β particle. Results from 14-MeV neutron irradiations (this study) and reactor fast-neutron irradiations (previous study) have shown that τ_n is dependent on the distance of the electron quasi-Fermi level E_{Fn}, below the edge of the conduction band. When $E_{Fn} \gtrsim 0.37$ eV ($\rho \gtrsim 2\times10^4$ Ω cm), τ_n is of the order of tens of msec. However, for $E_{Fn} \lesssim 0.37$ eV, τ_n is larger by a factor of $\sim 10^3$. The limiting position of E_{Fn} in fast-neutron-irradiated CdS is ≈ 0.37 eV, and depends on the induced defects as well as ionization. The large increase in τ_n with decreasing E_{Fn} probably arises because the process determining the occupancy of sensitizing centers changes from thermal-equilibrium kinetics to recombination kinetics. These centers are probably associated with fast-neutron-induced defects (or defect clusters). These results, in conjunction with a study of the changes in resistivity with fluence and the characteristics of thermal annealing, have shown that 14-MeV neutrons and reactor fast neutrons produce the same kinds of defects in CdS. Some unique features of these experiments were that resistivities were obtained in the range 10^1–10^6 Ω cm by radiation doping, and that τ_n was determined by self-ionization resulting from the β decay of radioisotopes. Also discussed are resistivity inhomogeneities in CdS, and γ-induced conductivity and photoconductivity experiments in fast-neutron-irradiated CdS.

INTRODUCTION

EFFECTS associated with the decay of radioisotopes in neutron-irradiated semiconductors can produce significant changes in the electrical properties.[1–3] Transmutation doping and nuclear recoil effects in semiconductors exposed to thermal neutrons have received much attention.[2–7] Less attention has been given to (1) examining effects associated with the absorption of radiation emitted from the excited nucleus, and (2) a study of these effects in fast-neutron-irradiated semiconductors. In some materials such effects may be either insignificant (e.g., the concentrations of radioisotopes may be small as a result of small reaction cross sections), or difficult to detect (e.g., it may be difficult to separate radioactive decay effects from effects associated with thermal annealing of neutron-induced defects). A recent study[1] of the effects of fast-neutron irradiation on the electrical properties of CdS has shown that ionization resulting from the β decay of radioactive isotopes can produce significant changes in the resistivity. The purpose of this study was to relate changes in the resistivity with time after fast-neutron irradiation to the measured decay of radioactivity from CdS.

In the previously reported study,[1] both low- and high-resistivity CdS single crystals (abbreviated as LRC and HRC throughout this text) were irradiated at room temperature in a reactor to fast-neutron fluences of 10^{14}–10^{17} neutrons/cm^2. (All further reactor-irradiation results mentioned in this paper are taken from Ref. 1.) Those studies showed that the Hall mobility decreased by 3–5 and 20–30% for fluences of 10^{14} and 10^{17} neutrons/cm^2, respectively. The crystals were still n type after irradiation to $>10^{17}$ neutrons/cm^2 and the resistivity (and electron quasi-Fermi level) approached a limiting value independent of the initial resistivity. Following irradiation, three separate time-dependent processes occurred which caused changes in the resistivity. One of these processes was temperature-dependent and was attributed to the annealing of radiation-induced defects. The other two processes were temperature-independent and were attributed to self-ionization resulting from radioactive decay. The major radioactive process was associated with the β decay from radioactive ^{32}P, and the other process was tentatively identified as resulting from the ^{115}Cd (2.3-day half-life) β decay. These radioactive isotopes were produced by (n,p) and (n,γ) reactions, respectively. The cross section for the ^{114}Cd$(n,\gamma)^{115}$Cd reaction was unknown, so the magnitude of the electrical changes associated with the two β decays could only be compared experimentally.

In this study similar effects were examined in both HRC and LRC irradiated with 14-MeV neutrons to fluences of 10^{10}–10^{13} neutrons/cm^2. Primary emphasis

† This work was supported by the U. S. Atomic Energy Commission.

[1] R. T. Johnson, Jr., J. Appl. Phys. **39**, 3517 (1968).
[2] J. H. Crawford, Jr., and J. W. Cleland, in *Radioisotopes in the Physical Sciences and Industry* (International Atomic Energy Agency, Vienna, 1962), Vol. 1, p. 269.
[3] J. W. Cleland, in *Radiation Damage in Solids*, edited by D. S. Billington (Academic Press Inc., New York, 1962), p. 384.
[4] H. C. Schweinler, J. Appl. Phys. **30**, 1125 (1959).
[5] G. K. Lindeberg, J. Appl. Phys. **38**, 3651 (1967).
[6] W. G. Clark and R. A. Isaacson, J. Appl. Phys. **38**, 2284 (1967).
[7] R. B. Oswald, Jr., and C. Kikuchi, Nucl. Sci. Eng. **23**, 354 (1965).

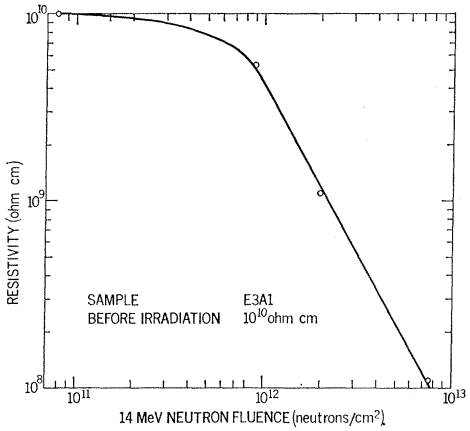

FIG. 1. Resistivity variations with 14-MeV neutron irradiation for high-resistivity (10^{10} Ω cm) CdS single crystals. These results were obtained by successive irradiations of sample E3A1. The resistivity was measured 1–2 days after irradiation, the time between irradiations was 2–4 days, and the entire series took 10 days. These are typical results obtained from high-resistivity homogeneous samples. Anomalous results were obtained for inhomogeneous samples.

was placed on studying HRC because they have small electron concentrations and are thus sensitive to ionization effects. The neutron-reaction cross sections for monoenergetic 14-MeV neutrons were accurately known, so measured changes in resistivity and surface radioactivity were compared with calculated decay rates. From these data, self-ionization effects resulting from the β decays of ^{115}Cd as well as ^{32}P were identified. Electron free lifetimes were determined from the induced conductivity resulting from self-ionization from radioactive decay for both 14-MeV and reactor-fast neutron-irradiated CdS. Fast-neutron-induced defect characteristics were determined by examining (1) the dependence of the electron free lifetime on the electron quasi-Fermi level position, (2) the changes in resistivity with fluence, and (3) the properties of room-temperature annealing. Resistivity inhomogeneities in CdS are discussed in Appendix A. γ-induced conductivity and photoconductivity experiments are discussed in Appendix B.

EXPERIMENTAL TECHNIQUE

Single crystals with dark resistivities in the ranges 1–10 Ω cm (LRC) and 10^7–10^{10} Ω cm (HRC) were used. The dimensions of samples used for electrical measurements were approximately 6×6×1 mm, whereas the sample used for the radioactivity measurements had approximate dimensions of 13×13×1.4 mm. The "c" axis was perpendicular to the major face. For electrical measurements particular attention was given to selecting samples which were relatively free of resistivity inhomogeneities. The method used for selecting these samples is discussed in Appendix A. The dark resistivities of HRC were determined after the samples equilibrated in the dark for at least 18–24 h. Other sample characteristics and the 4-terminal technique used for electrical measurements have been previously described.[1]

Neutrons with energies of 14.3 MeV were produced via the ^{3}H(^{2}H,n)^{4}He reaction using a Kaman Nuclear (Model A-1001) Neutron Generator, operating at an accelerating potential of 170 kV. The neutron flux was approximately 2×10^9 neutrons/cm^2 sec. The samples were irradiated at room temperature and were oriented so that the primary neutron beam was perpendicular to the major face. The neutron fluence was determined using sulfur dosimetry. The dosimetry analysis was performed by the Radiation Division at Sandia Laboratories.

For radioactivity measurements the irradiated sample was set in a stainless-steel planchet and placed within a lead shield with the major face of the crystal 2 cm from an end window (1.3 mg/cm^2) of a Geiger-Müller (GM) Detector. The operating voltage was 1200 V and was in the middle of the voltage plateau. The GM-tube pulses were passed to an ORTEC counting system consisting of: active filter amplifier, strobed single-channel analyzer, scaler, timer, and print-out control. Counts of 10^3 sec each were recorded by digital print-out and were taken continuously from 10 min after irradiation to 35 days after irradiation. The background of the counting system was 0.2 counts/sec.

EXPERIMENTAL RESULTS

Electrical Measurements

High-resistivity samples were irradiated with 14.3-MeV neutrons to fluences of 10^{10}–10^{13} neutrons/cm^2. Typical resistivity variations with fluence are shown in Fig. 1 for irradiated homogeneous samples. Anomalous results were obtained for inhomogeneous samples (i.e., the resistivity changes with fluence could not be fitted with a smooth curve). Only results obtained on irradiated-homogeneous samples will be presented and discussed further in this paper.

The results in Fig. 1 were obtained by successive irradiations of sample E3A1. The resistivity was measured 1–2 days after each irradiation and the time between irradiations was 2–4 days. The entire series took 10 days. The resistivity of 10^{10} Ω cm samples began to decrease significantly for fluences of 10^{11} neutrons/cm^2, and continued to decrease with increasing fluence. After irradiation to 10^{13} neutrons/cm^2 the resistivity was in the 10^7–10^8 Ω cm range. These results can be correlated with those obtained with reactor-irradiated samples. Extrapolation of the data in Fig. 1 to fluences of 10^{14} neutrons/cm^2 shows that the resistivity approaches 10^6–10^7 Ω cm. This is the same range of resistivities observed for HRC irradiated to the same fluence with reactor-fast neutrons.

Several LRC were irradiated with 14.3-MeV neutrons to 10^{13} neutrons/cm^2 and no change in either the

resistivity or Hall mobility was detectable. This is also in agreement with the reactor-irradiation results, which showed that such changes were only significant after irradiation to fluences $>10^{14}$ neutrons/cm^2.

The resistivity of the irradiated samples varied with time after irradiation. The results obtained from sample E3A1 are shown in Fig. 2. The time plotted in this figure is the time after the last irradiation in the series shown in Fig. 1. After irradiation the resistivity increased with time toward the pre-irradiation value and reached a constant value of $\sim 2\times 10^9$ Ω cm at 120–140 days after irradiation. These results are similar to those obtained for reactor-irradiated HRC except that at later times the resistivity of those samples continued to increase toward the pre-irradiation value with a dependence which varied exponentially with time. [Note that the reactor irradiated samples had been heavily irradiated (10^{17} neutrons/cm^2) and the resistivities after irradiation were in the 10^5–10^6 Ω cm range.]

Radioactivity Measurements

The sample used for radioactive decay measurements was cut from the same crystal as sample E3A1 which was used for the electrical measurements (see Figs. 1 and 2). The sample was irradiated to a fluence of 2.7×10^{13} neutrons/cm^2. The radioactivity data are given in Fig. 3. Curve A of this figure is the measured counts/sec as a function of time after irradiation. Curve B was obtained by subtracting out the straight-line portion (dashed) and replotting the initial points. Only representative data points are recorded here, although data were recorded continuously. These results show that for the period beginning 1 day after irradiation there are 2 primary decay processes which have half-lives of 2.3 and 14 days, and are thus associated with the decays of radioactive ^{115}Cd and ^{32}P, respectively.

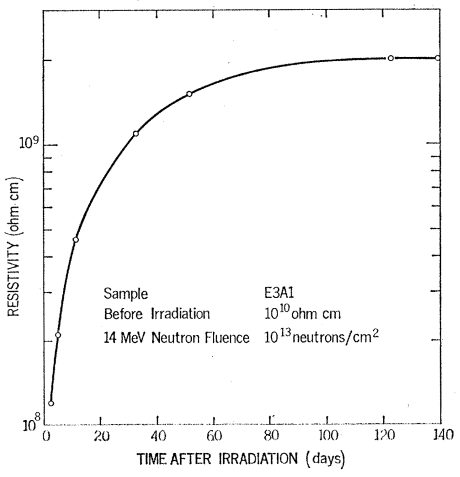

FIG. 2. Resistivity variations with time after 14-MeV neutron irradiation for high-resistivity CdS single crystals irradiated to 10^{13} neutrons/cm^2. These results were obtained from the same sample used in the series of irradiations given in Fig. 1. Plotted is the resistivity versus time after the last irradiation in that series.

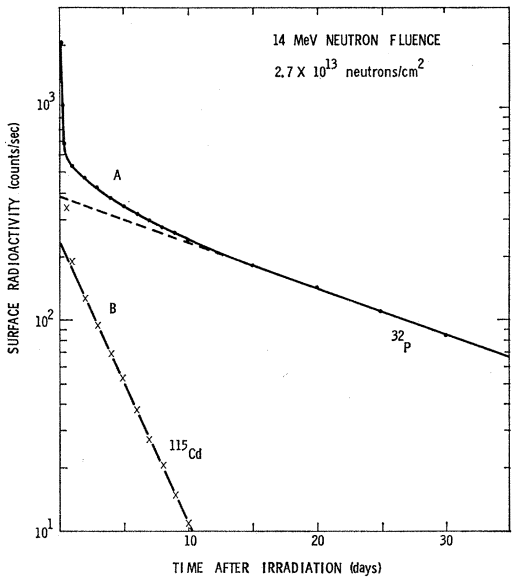

FIG. 3. Surface radioactivity from a CdS crystal as a function of time after 14-MeV neutron irradiation. This sample was cut from the same crystal as sample E3A1, which was used for the electrical measurements shown in Figs. 1 and 2. Curve A is the measured (counts/sec) versus time after irradiation. Curve B was obtained by subtracting out the straight-line portion and replotting the initial points. Only representative data points are recorded here, although data were recorded continuously. The results show that for the period $>$ 1 day after irradiation there are two primary decay processes. The predominant radioisotopes are ^{115}Cd and ^{32}P, which decay with half-lives of 2.3 and 14 days, respectively.

ANALYSIS AND DISCUSSION

Neutron Reactions

Neutrons undergo scattering and absorption (or capture) reactions with atomic nuclei. Each individual process in a particular target material is characterized by a macroscopic cross section Σ, which has units of cm^{-1}. For a particular process (or reaction), the total number of interactions A_0 per cm^3 of target material produced by neutron irradiation, is given by

$$A_0=\Sigma\phi, \qquad (1)$$

where ϕ is the neutron fluence (neutrons/cm^2).

For fast-neutron irradiations the most important process which produces atomic displacements is elastic scattering. The macroscopic elastic scattering cross section for 14-MeV neutrons in CdS is $\sim 7\times 10^{-2}$ cm^{-1}. Thus, the total number of primary interactions (interactions between incident neutrons and lattice atoms) for a fluence of 10^{13} neutrons/cm^2 is $\sim 7\times 10^{11}$ cm^{-3}. The primary recoil produces further atomic displacements, and this displacement cascade accounts for most of the defects produced during fast-neutron irradiation. Estimates show that there is a total of $\sim 2\times 10^{16}$ displace-

TABLE I. Principal nuclear reactions and recoil nuclei produced as a result of 14-MeV neutron irradiation in CdS. Also given are the decay schemes (half-lives and characteristic β and γ radiations), the product of the macroscopic cross section (Σ) and the decay constant (λ), and the estimated concentrations of recoil nuclei for a fluence of 10^{13} neutrons/cm^2.

Reaction	Half-life	Characteristic radiation, energy (MeV) β	γ	$\Sigma\lambda$ (cm sec)$^{-1}$	Concentration of recoil nuclei for $\phi=10^{13}n/\text{cm}^2$, (cm^{-3})
^{32}S $(n,\alpha)^{29}$Si	Stable	. . .	. . .	. . .	2×10^{10}
^{34}S $(n,\alpha)^{31}$Si	2.7 h	1.5	1.3	8×10^{-9}	1×10^{9}
^{112}Cd $(n,\alpha)^{109}$Pd	13.6 h	1.0	0.1–0.8	2×10^{-10}	2×10^{8}
^{34}S $(n,2n)^{33}$S	Stable	. . .	. . .	. . .	1×10^{9}
^{106}Cd^{m} $(n,2n)^{105}$Cd	55 min	0.8,1.7	0.03–2.3	4×10^{-8}	2×10^{9}
$^{111-114}$Cd $(n,2n)$	Stable	. . .	. . .	. . .	2×10^{11}
^{116}Cd $(n,2n)^{115}$Cd	43 days	0.7,1.6	0.5–1.3	2×10^{-10}	1×10^{10}
	2.3 days	0.58,1.11	0.2–0.7	5×10^{-9}	1×10^{10}
^{32}S $(n,p)^{32}$P	14.3 days	1.71	None	3×10^{-9}	5×10^{10}
^{112}Cd $(n,p)^{112}$Ag	3.2 h	1.0–4.1	0.6–3.3	3×10^{-9}	5×10^{8}
^{113}Cd $(n,p)^{113}$Ag	5.3 h	2.0	0.1–1.2	4×10^{-9}	1×10^{9}

ments/cm^3 which result from a 14-MeV neutron fluence of 10^{13} neutrons/cm^2 in CdS. Not all of this damage, especially close interstitial-vacancy pairs, is stable at room temperature. This is concluded from recent experiments by Vook,[8] which have shown that most electron-irradiation-induced defects in CdS anneal well below room temperature. As was seen in the reactor irradiation experiments the more stable defects (or defect-impurity complexes) at room temperature affect the electrical properties. The 14-MeV neutron-irradiation experiments have shown that the change in resistivity with fluence (Fig. 1) is consistent with the changes observed in the reactor irradiation experiments. Although some of these effects are associated with radioactive decay, the results do suggest that 14-MeV and reactor fast neutrons produce the same kinds of defects in CdS. Stein[9] has shown that this is also the case for n-type Si.

Effects resulting from neutron absorption reactions are also important. The most important 14-MeV neutron reactions in CdS are given in Table I. Also given are the concentrations of recoil nuclei (either stable isotopes or radioisotopes) produced by a 14-MeV neutron fluence of 10^{13} neutrons/cm^2, and the decay schemes (half-lives and characteristic β and γ radiations) for the radioisotopes. The most important reactions in CdS for 14-MeV neutrons are the $(n,2n)$, (n,p), and (n,α) reactions; whereas the (n,γ) as well as the (n,p), and (n,α) reactions are of most significance for reactor-energy neutrons ($\sim$0.1 to $\sim$10 MeV). The most important radioisotopes in both the reactor and 14-MeV neutron-irradiation experiments are ^{115}Cd and ^{32}P. The ^{32}P radioisotope results from an (n,p) reaction in both cases; however, ^{115}Cd results from an (n,γ) reaction for reactor neutrons and an $(n,2n)$ reaction for 14-MeV neutrons.

[8] F. L. Vook, Appl. Phys. Letters **13**, 25 (1968).
[9] H. J. Stein, J. Appl. Phys. **38**, 204 (1967).

Radioactive Decay

The number of atoms A per unit volume of a given radioisotope at a particular time, is given by

$$A=A_0e^{-\lambda t}, \tag{2}$$

where λ is the decay constant and t is the time after irradiation (assuming that all A_0 nuclei were produced at the same time, $t=0$). Both the measured radioactivity and the electrical changes associated with the radioactive-decay processes are functions of the rate of decay, which is given by

$$dA/dt=-\lambda\Sigma\phi e^{-\lambda t}. \tag{3}$$

The initial decay rates ($t=0$) for various radioisotopes are compared in Table I by examining the product $\Sigma\lambda$. This product is dependent only on material characteristics. The results show that the largest $\Sigma\lambda$ product is associated with the ^{106}Cd$(n,2n)^{105}$Cd reaction and that the ^{105}Cd radioisotope has a half-life of 55 min. Effects related to the decay of this radioisotope are significant for only the first few hours after irradiation. The radioisotopes listed in Table I with half-lives <1 day account for the large initial count rate observed in Fig. 3. Of the radioisotopes with half-lives >1 day, the results in Table I show that the 2.3-day ^{115}Cd and 14.3-day ^{32}P decays are the most significant, in agreement with the radioactivity measurements (Fig. 3). No effects from the 43-day ^{115}Cd decay were detectable in either the resistivity or radioactivity data. Throughout the remainder of this paper a reference to the ^{115}Cd decay implies the 2.3-day half-life process.

In order to correlate the radioactivity measurements with the electrical changes, the data in Fig. 3 for the period >1 day after irradiation were corrected for counting efficiencies. These were determined from the counts/sec data, the sample mass, the neutron fluence, the decay rates, and the known neutron reaction cross

sections. The counting efficiencies were 0.9% for ^{115}Cd and 2.3% for ^{32}P. This correction has the effect of shifting the ^{115}Cd curve (curve B, Fig. 3) with respect to the ^{32}P curve (Fig. 3). The resulting ratio of the ^{115}Cd and ^{32}P intercepts with the $t=0$ axis is just $(\Sigma\lambda)_{^{115}Cd}/(\Sigma\lambda)_{^{32}P}$, which is a factor of 1.7. The results, shown in Fig. 4(b), give the disintegrations per sec as a function of time for the sample used for the radioactivity measurements.

Induced-Conductivity Data

The electrical changes with time after irradiation were analyzed by converting the resistivity (ρ) data for sample E3A1 (Fig. 2) to conductivities, $\sigma=1/\rho$, since it is σ that is proportional to the electron concentration n. It was assumed that the Hall mobility of this sample did not change as a function of either the fluence or the time after irradiation since such changes were not observed in similarly irradiated LRC. Thus changes in σ reflect changes in n.

The data in Fig. 2 show that the resistivity approached a constant value of $\rho_c=2\times10^9$ Ω cm at ~120 days following irradiation; the corresponding limiting conductivity was $\sigma_c=5\times10^{-10}(\Omega\text{ cm})^{-1}$. The difference $\sigma-\sigma_c$ was taken to be the change in conductivity resulting from the time-dependent processes. The parameter $\sigma-\sigma_c$ as a function of time after irradiation was determined from the data in Fig. 2. The results are given in Fig. 4(a), curve A. Curve B was obtained by subtracting out the straight-line portion and replotting the initial points. These results show that the conductivity changes can result from two processes which vary exponentially with time. The rate constants determined from these data are 0.33/day and 5.0 $\times10^{-2}$/day and correspond to processes which decay with half-lives of 2.1 and 14 days, respectively. These are the half-lives (within experimental error) associated with the radioactive decay of ^{115}Cd and ^{32}P.

Changes in the electrical properties with time after irradiation can result from the changing concentrations of the radioisotopes, the recoil from the decay, and effects associated with the nuclear radiations. The concentrations of the radioisotopes produced by 14-MeV neutron irradiation to fluences of 10^{13} neutrons/cm^2 are given in Table I. The values of these concentrations are much less than is normally required for chemical doping and thus do not account for the observed electrical changes. These conclusions are in agreement with the experimental work of Blount *et al.*[10] on ZnS. They introduced total impurity concentrations of 10^{13} cm^{-3} through radioactive decay of ^{35}S in high-resistivity material and found no change in the dark conductivity. Lattice damage can be produced as a result of nuclear recoil as well as nuclear radiation. However, much of this damage is in the form of vacancy-interstitial pairs and is not expected to be stable at room temperature.[8] Ionization[11] (generation of electron-hole pairs) can be produced by the radiations emitted in radioactive decay as well as by the recoiling nucleus.[12] Estimates show that the energy carried by the recoiling nucleus in these experiments (~77 eV for a ^{32}P recoil) is insignificant compared to the energy deposited by the nuclear radiation. The predominant effect is ionization by the nuclear radiations producing conduction electrons, which cause a decrease in resistivity (or increase in conductivity). As the intensity of nuclear radiation decreases with decreasing radioisotope concentration, fewer carriers are generated so the resistivity increases (or conductivity decreases). This interpretation is further substantiated by observations of induced conductivity in CdS by other experimenters while irradiating with high-energy electrons[13–17] (including β particles), as well as with γ rays

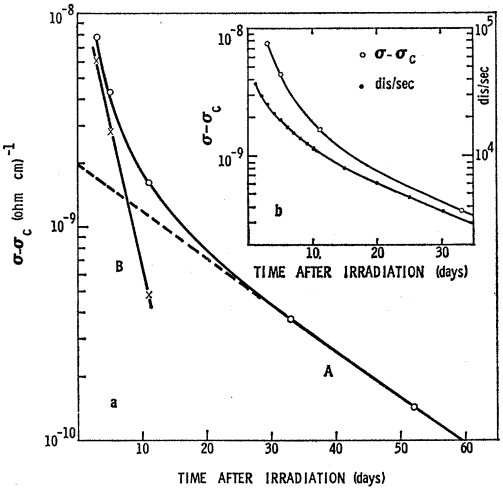

FIG. 4. Change in conductivity with time after irradiation (Sec. a) and comparison with measured radioactivity (Sec. b). In (a), curve A is σ-σ_c versus t, where σ is the measured conductivity at time t, and σ_c is the time-independent (constant) limiting conductivity. This graph was obtained from an analysis of the data in Fig. 2 for sample E3A1. Curve B was obtained by subtracting out the straight-line portion and replotting the initial points. The rate constants for the two exponential variations are the same as those obtained from the radioactivity data. The insert (b) gives a comparison between the σ-σ_c data and the radioactive decay data (disintegrations/sec) versus t. The radioactivity results were determined from the data given in Fig. 3 and from the analysis outlined in the text. The difference in the early time variations is due to room-temperature annealing, which varies exponentially with approximately the same rate constant as the ^{115}Cd decay.

[10] G. H. Blount, P. B. P. Phipps, and R. H. Bube, J. Appl. Phys. **38**, 4550 (1967).

[11] G. Dearnaley and D. C. Northrop, *Semiconductor Counters for Nuclear Radiations* (Wiley-Interscience, Inc., New York), 1st ed. (1963), pp. 115–117, 2nd ed. (1966), pp. 19–24, 340–341.

[12] A. R. Sattler, in *Radiation Effects in Semiconductors*, edited by F. L. Vook (Plenum Publishing Corp., New York, 1968), p. 243.

[13] C. E. Bleil, D. D. Snyder, and Y. T. Sihvonen, Phys. Rev. **111**, 1522 (1958).

[14] S. Takagi and T. Suzuki, Acta Cryst. **8**, 441 (1955).

[15] S. Ibuki, J. Phys. Soc. Japan **14**, 1196 (1959).

[16] S. V. Svechnikov, Zh. Tekhn. Fiz. **26**, 1646 (1956) [English transl.: Soviet Phys.—Tech. Phys. **1**, 1601 (1957)].

[17] R. Frerichs, Phys. Rev. **72**, 594 (1947); **76**, 1869 (1949); J. Appl. Phys. **21**, 312 (1950).

TABLE II. Characteristics of the ^{115}Cd and ^{32}P continuous β-ray spectra.[a] Given is the maximum energy (E_m), the average energy (E_{av}), and the apparent mass-absorption coefficient[b] (μ_m) for each spectrum.

Isotope	β energy (MeV) E_m	E_{av}	Mass-absorption coefficient, μ_m(cm^2/g)
^{115}Cd	0.58 (42%)	0.23	32
	1.11 (58%)	0.44	15
^{32}P	1.71	0.70	9

[a] The ^{115}Cd β spectrum with E_m=0.58 MeV is observed 42% of the time and the E_m=1.11 MeV spectrum is observed 58% of the time.
[b] Determined using Eq. (4) in the text.

and x rays.[15–24] This is the same conclusion as was obtained from the reactor-irradiation experiments.

The change in conductivity, $\sigma-\sigma_c$, with time after irradiation and the radioactivity data are compared in Fig. 4(b). The results show that the contribution due to the 2-day half-life process relative to the 14-day half-life process is considerably greater in the $\sigma-\sigma_c$ data than was observed in the radioactivity data. It must also be remembered that the sample used for electrical measurements was irradiated in a series of exposures which took 10 days, and the electrical measurements versus time after irradiation (Fig. 2) were not initiated until the last irradiation in that series. Thus both the ^{115}Cd and ^{32}P radioisotopes produced during the early irradiations had decayed considerably (especially ^{115}Cd) by the time the last irradiation had been completed. Thus, the time $t=0$ given in Figs. 2, 4(a), and 4(b) is not the time at which all the ^{115}Cd and ^{32}P radioisotopes were produced. Analysis of the data showed that the ^{115}Cd and ^{32}P radioisotopes at $t=0$ were only 62 and 91%, respectively, of the values determined using Eq. (1). Combining these results with the $\sigma-\sigma_c$ data (intercepts of 2-day and 14-day half-life processes with the $t=0$ axis) and the radioactivity data (ratios of $\Sigma\lambda$ for ^{115}Cd and ^{32}P) showed that the contribution to the conductivity by the 2-day half-life process relative to the 14-day half-life process is a factor of 7 greater than the same ratio observed in the radioactivity data. There are several possible effects which may account for this difference.

Counting Efficiencies

The counting efficiencies for the ^{115}Cd and ^{32}P radiations could be incorrect. The most likely source of error would be the values of the neutron-reaction cross sections. This information was used to correct the measured radioactivity data (counts/sec versus t) (Fig. 3) resulting in the data (dis/sec versus t) given in Fig. 4(b). The authors have no reason to doubt the accuracy of the cross-section data, and thus conclude that this does not account for the differences in conductivity and radioactivity data.

Ionization

Differences in the ionization produced by the different radiations emitted from the various radioisotopes could also be significant. The radiation-ionization energy ϵ (average amount of energy given up by high-energy radiation in the process of generating an electron-hole pair[25]), is not significantly dependent on either the type or the energy of the radiation.[11,24–26] Thus, ionization effects associated with the different radiations from radioactive decay can be compared by examining the relative amount of energy deposited in the material.

Some of the characteristics of the continuous β-ray spectra[27,28] from ^{115}Cd and ^{32}P are given in Table II. The ^{115}Cd radioisotope has two different β-decay schemes. The β spectrum with a maximum energy (E_m) of 0.58 MeV is emitted 42% of the time while the E_m=1.11-MeV spectrum is observed 58% of the time. The average energies (E_{av}) of these spectra are 0.23 and 0.44 MeV, respectively. γ rays with energies 0.2–0.7 MeV are also emitted as a result of the ^{115}Cd decays. In contrast, the ^{32}P radioisotope is characterized by a single β decay (E_m=1.71 MeV), and has no γ-ray emission. Estimates for these β spectra in CdS show that $\lesssim$4% of the absorbed energy results in bremsstrahlung[28] and electron-atom collisions.[29] Most of the absorbed β energy and γ energy (absorbed primarily through Compton scattering) results in ionization (i.e., through interactions with electrons in the semiconductor producing electron-hole pairs).[11,26,28,29]

Consider first effects associated with the different β radiations. The absorption of a continuous β-ray spectrum can be approximated by an exponential function, in contrast to the monoenergetic case where the range of the particle is specified. An apparent mass-absorption coefficient μ_m (linear-absorption coefficient

[18] I. D. Konozenko, V. I. Ust'yanov, and A. P. Galushka, Fiz. Tverd. Tela **2**, 1584 (1960) [English transl.: Soviet Phys.—Solid State **2**, 1436 (1961)].
[19] P. G. Litovchenko and V. I. Ust'yanov, Fiz. Tverd. Tela **4**, 1689 (1962) [English transl.: Soviet Phys.—Solid State **4**, 1241 (1963)].
[20] P. G. Litovchenko, I. D. Konozenko, and V. I. Ust'yanov, Fiz. i Tekhn Poluprovodnikov **1**, 491 (1967) [English transl.: Soviet Phys.—Semiconductors **1**, 407 (1967)].
[21] H. Ikawa, O. Matumura, and H. Suzuki, Japan. J. Appl. Phys. **1**, 236 (1962).
[22] C. G. Clayton, B. C. Haywood, and J. F. Fowler, Nature **183**, 1112 (1959).
[23] T. Y. Sera, V. V. Serdyuk, and I. M. Shevchenko, Fiz. Tverd. Tela **3**, 3537 (1961) [English transl.: Soviet Phys.—Solid State **3**, 2568 (1962)].
[24] S. V. Svechnikov and V. G. Chalaya, Fiz. Tverd. Tela **8**, 3108 (1966); **7**, 3413 (1965) [English transls.: Soviet Phys.—Solid State **8**, 2486 (1967); **7**, 2750 (1966)].
[25] C. A. Klein, J. Appl. Phys. **39**, 2029 (1968).
[26] W. L. Brown, IRE Trans. Nucl. Sci. **1**, 2 (1961).
[27] D. Strominger, J. M. Hollander, and G. T. Seaborg, Rev. Mod. Phys. **30**, 585 (1958).
[28] R. D. Evans, *The Atomic Nucleus* (McGraw-Hill Book Co., New York, 1955), pp. 567, 617–619, 625–629.
[29] J. W. Corbett, *Electron Radiation Damage in Semiconductors and Metals* (Academic Press Inc., New York, 1966), pp. 17–22, 35, 36.

divided by the density of the absorber) for a particular spectrum can be determined using the empirical expression[28]

$$\mu_m = 17/E_m^{1.14}\ \mathrm{cm^2/g}, \quad (4)$$

where E_m is in MeV. The calculated values of μ_m for the ^{115}Cd and ^{32}P β spectra are given in Table II. The thickness of a CdS absorber required to reduce the β-ray intensity to one-tenth its original value ranges from 0.15–0.5 mm for spectra with E_m ranging from 0.58–1.71 MeV. (This can be compared to a range of 1.7 mm for monoenergetic 1.7-MeV β particles.) For samples with the dimensions of those used in these experiments estimates have shown that a large fraction of the β energy is absorbed in the sample. This, of course, accounts for the low counting efficiencies observed in the radioactivity measurements. The average energy deposited as a result of absorption of β-rays from a ^{32}P decay is larger than that resulting from either of the ^{115}Cd β decays. However, initially there are $\sim$1.7 times as many ^{115}Cd decays as ^{32}P decays. Estimates show that initially the rate of energy absorption is approximately the same for the ^{32}P and ^{115}Cd β decays. A similar conclusion is reached when considering effects that can result from the γ radiation. The ^{115}Cd radioisotope emits γ radiation whereas the ^{32}P radioisotope does not. The absorption coefficient for these γ rays have a maximum value of $\sim$0.4 cm^2/g, and in comparison to the β-absorption coefficients (Table II) it is concluded that γ-ray effects are not significant. This is in agreement with the work of Ibuki.[15] He examined induced conductivity from both β and γ radiation in CdS and found that γ effects were $<1\%$ of the β-radiation effects. It is concluded from these results that the differences in the conductivity and radioactivity data cannot be explained on the basis of energy absorbed from the different β decays.

Annealing

Electrical changes associated with the thermal annealing of fast-neutron-induced defects may account for the differences in the conductivity and radioactivity data. Results from the reactor-irradiation experiments showed that room-temperature annealing of neutron-induced defects was characterized by rate constants λ_a, which depended on either the defect concentration or the position of the electron quasi-Fermi level E_{Fn} with respect to the edge of the conduction band. Since the resistivity-versus-fluence data showed that the induced defects in 14-MeV and reactor-neutron-irradiated CdS are approximately the same, then the annealing characteristics should also be similar.

Consider first the dependence of $|\lambda_a|$ on the defect concentration. For sample E3A1 (Figs. 1 and 2) the $|\lambda_a|$ would be $<10^{-4}$/day, as determined from the reactor-irradiation results. For a rate constant of this magnitude no significant changes in resistivity would be detected over the entire 140-day period after irradiation. This is consistent with the observation in Fig. 2 that any resistivity changes due to annealing over the period from 120–140 days after irradiation must be within experimental error. The more interesting case to consider is the dependence of $|\lambda_a|$ on E_{Fn}. The reactor-irradiation results showed that $|\lambda_a|$ varied from 10^{-4}–10^{-2}/day as E_{Fn} varied from 0.1–0.4 eV (the resistivity varied from 10^0–10^5 Ω cm). When these data are plotted ($|\lambda_a|$ versus E_{Fn}) and extrapolated to $E_{Fn}\approx 0.59$ eV ($\rho = 10^8$ Ω cm) for sample E3A1 (Figs. 1 and 2), it was found that $|\lambda_a|$ was in the range of 0.3/day. This is the same as the rate constant for the ^{115}Cd decay. Thus, defect annealing could account for the difference between the conductivity and radioactivity data.

These results suggest that (1) λ_a is more dependent on E_{Fn} than on the defect concentration, and (2) that there are two processes with half-lives of 2 days causing changes in the electrical properties. One of these processes certainly results from the radioactive decay of ^{115}Cd and the other results from thermal annealing of neutron-induced defects. It should be possible to separate these processes either by examining the temperature dependence (defect annealing is temperature-dependent, whereas radioactive decay is not) or by irradiating HRC to different resistivities, thus varying λ_a. In order to compare results from different samples in such experiments, the samples should have the same initial resistivity. The experiments have not yet been attempted because of difficulties encountered in selecting high-resistivity-homogeneous samples with similar electrical properties.

Induced-Conductivity Mechanism

In these experiments most of the β energy from radioactive decay was absorbed in the samples and the energy was lost predominantly through processes associated with ionization. It is of interest to compare ionization effects with the observed electrical changes. Consider first the rate of ionization. The rate of β emission (β particles per cm^3 sec) is given by $(-dA/dt)$; see Eq. (3). Assume that all of the energy is dissipated through ionization and that the average energy loss per β particle is E_{av}. Then the number of electron-hole pairs generated per sec per unit volume, g, by ionization is given by

$$g = (E_{av}/\epsilon)(-dA/dt). \quad (5)$$

This equation was evaluated for the ^{32}P decay in sample E3A1, at $t=0$. The data in Figs. 1 and 2, the data in Tables I and II, and the value[11,25] $\epsilon = 7.3$ eV were used. The electron-hole generation rate from ionization was found to be $g\approx 3\times 10^9$ (electron-hole pairs)/cm^3 sec.

The change in conductivity, $\Delta\sigma$, in semiconductors (or insulators) which results from the absorption of radiation is given by

$$\Delta\sigma = e(\Delta n\mu_n + \Delta p\mu_p), \quad (6)$$

TABLE III. Electron free lifetimes[a] τ_n, determined from induced conductivity resulting from the β decay of ^{32}P in fast-neutron-irradiated CdS. Given for each sample is the fast-neutron fluence, the resistivity before irradiation and at ~1 day after irradiation, and the initial electron-hole generation rate[b] (g).

Sample	Neutron fluence (>3 MeV) (neutrons/cm²)	Resistivity: Before irradiation	Resistivity: After irradiation (Ω cm)	g (cm³ sec)⁻¹	τ_n (sec)
E3A1	1×10^{13} [c]	HRC[d]	1×10^{8}	3×10^{9}	15×10^{-3}
C-9D	2×10^{16}	HRC	2×10^{5}	6×10^{12}	11×10^{-3}
1B1A2	2×10^{16}	HRC	9×10^{4}	6×10^{12}	24×10^{-3}
H1B3	1×10^{15}	LRC	4×10^{3}	3×10^{11}	6
C1B3	1×10^{15}	LRC	3×10^{3}	3×10^{11}	7
C1D3	1×10^{15}	LRC	3×10^{3}	3×10^{11}	9
C1D4	1×10^{15}	LRC	2×10^{3}	3×10^{11}	14
H1B6	4×10^{14}	LRC	1×10^{3}	1×10^{11}	45
E1C2	3×10^{15}	LRC	2×10^{2}	1×10^{12}	50

[a] Determined using Eq. (9) in text.
[b] Determined using Eq. (5) in text.
[c] Sample E3A1 was irradiated with 14-MeV neutrons; all other samples were irradiated with reactor-fast neutrons.
[d] HRC denotes high-resistivity crystals (10^{7}–10^{10} Ω cm) and LRC denotes low-resistivity crystals (1–10 Ω cm).

where Δn and Δp are the change in electron and hole concentrations, μ_n and μ_p are the electron and hole mobilities, and e is the electronic charge. In deriving Eq. (6), the assumption was made that changes in mobility were negligible. This is a valid assumption for these experiments. Since g is the ionization rate per unit volume, the change in the electron and hole concentrations can be expressed as

$$\Delta n = g\tau_n \quad \text{and} \quad \Delta p = g\tau_p, \tag{7}$$

where τ_n and τ_p are the free lifetimes[30] of the electrons and holes, respectively. Thus, $\Delta\sigma$ can be expressed as

$$\Delta\sigma = eg(\mu_n\tau_n + \mu_p\tau_p). \tag{8}$$

For an n-type semiconductor like CdS, where $\mu_n\tau_n \gg \mu_p\tau_p$, Eq. (8) reduces to

$$\Delta\sigma = eg\mu_n\tau_n. \tag{9}$$

The induced conductivity from the radioactive decay of ^{32}P in sample E3A1 (Fig. 4) was analyzed using Eq. (9). The electron free lifetime was determined by using Eqs. (5) and (9), and by assuming $\mu_n = 300$ cm²/V sec. (This assumption was based on the results obtained from Hall mobility measurements in the reactor-irradiation experiments.) The calculations showed that $\tau_n = 15$ msec. The results from this analysis are summarized in Table III. Electron free lifetimes of the order of msec have frequently been observed by other investigators in optical experiments using high-resistivity photosensitive CdS.[30–32] In many optical experiments most of the energy is absorbed in the surface of the sample. Bube[32] has shown that τ_n for surface excitation in CdS is smaller than that for volume excitation owing to a higher rate of recombination at the surface. Similar effects have been observed using more highly ionizing radiations in other materials.[33] In the experiments reported here the excitation is truly a volume effect because the decaying radioisotopes are randomly distributed throughout the crystal. It is expected then that the τ_n calculated here would be somewhat higher than that determined from optical experiments. It is concluded from these results that induced conductivity from ionization resulting from radioactive decay in CdS can be described analytically using Eq. (9).

The data from two reactor-irradiated HRC[1] were analyzed in the same manner. The results are summarized in Table III. The calculated τ_n were within a factor of 2 of the value reported herein for the HRC irradiated by 14-MeV neutrons. It should be noted that HRC were irradiated with reactor-fast neutrons to fluences of 10^{16} neutrons/cm² [>3 MeV, which is the threshold for the $^{32}S(n,p)^{32}P$ reaction], and with 14-MeV neutrons to fluences of 10^{13} neutrons/cm². A factor-of-2 variation in τ_n for these irradiations is considered to be a small variation considering (1) the wide range of fluences, (2) that g varied from $\sim3\times10^{9}$ to $\sim6\times10^{12}$/cm³ sec, and (3) that the resistivities after irradiation were 10^{5}–10^{8} Ω cm. (Note that these results are consistent with the previous observation that the same kinds of defects are introduced by 14-MeV and reactor-fast neutrons.)

Similar analysis of six reactor-irradiated LRC[1] gave values of τ_n of the order of tens of seconds. These lifetimes are $\sim10^{3}$ times those of the irradiated HRC. The LRC that were analyzed had been irradiated to fluences of 10^{14}–10^{15} neutrons/cm² (>3 MeV). The resistivities after irradiation ranged from 10^{2}–10^{3} Ω cm. The results for the LRC, given in Table III, also show that τ_n increased with decreasing resistivity.

These data were further analyzed by examining the dependence of τ_n on the position of E_{Fn} below the

[30] R. H. Bube, *Photoconductivity of Solids* (Wiley-Interscience, Inc., New York, 1960), pp. 56–74, 77, 287; in *Physics and Chemistry of II–VI Compounds*, edited by M. Aven and J. S. Prener (Wiley-Interscience, Inc., New York, 1967), pp. 657–705.
[31] R. H. Bube, AIME Trans. Met. Soc. **239**, 291 (1967).
[32] R. H. Bube, Phys. Rev. **101**, 1668 (1956).
[33] J. M. Taylor, *Semiconductor Particle Detectors* (Butterworth and Co., Ltd., London, 1963), pp. 25, 28, 45.

edge of the conduction band at ~1 day following irradiation. E_{Fn} was determined from the measured resistivities and Hall mobilities of the samples given in Table III following the method previously outlined.[1] The results are given in Fig. 5 and show that the shorter lifetimes were observed for $E_{Fn} \gtrsim 0.37$ eV and the longer lifetimes for $E_{Fn} \lesssim 0.37$ eV. $E_{Fn} \approx 0.37$ eV is the limiting position of E_{Fn} in fast-neutron-irradiated CdS and depends on induced defects as well as ionization effects. [The reactor-irradiation experiments showed that E_{Fn} decreased for the irradiated LRC and increased for the irradiated HRC. Highly irradiated samples all approached the limiting position of E_{Fn} (limiting $\rho \approx 2 \times 10^4$ Ω cm).] These results further show that τ_n varies from ~15 msec to ~50 sec as E_{Fn} decreases and shifts through the limiting position of E_{Fn}. The dependence of τ_n on E_{Fn} was also confirmed by independent experiments on γ-induced conductivity and on photoconductivity in neutron-irradiated and unirradiated CdS samples. These experiments are discussed in Appendix B.

Trapping effects in CdS are responsible for long response times (i.e., rise and decay times, denoted as τ_0) for induced conductivity from ionizing radiations. (A trapping center is here defined as a center whose occupancy is determined by thermal equilibrium with the nearest band.) The shortest time to readjust to abrupt changes in conductivity occurs when trapping effects are insignificant and $\tau_0 = \tau_n$. When trapping effects are important, $\tau_0 > \tau_n$. In the case of electron traps, for example, τ_0 is very dependent on the density of trapped electrons near the electron quasi-Fermi level. Response times of the order of minutes and longer have been frequently observed in unirradiated CdS (neutron irradiation) in studies of induced conductivity from γ radiation,[11,15–20,33] β radiation,[14,15] α-particle radiation,[11] and visible radiation,[30] especially for low-ionization intensities. Long response times have also been observed in experiments on γ-induced conductivity and photoconductivity in neutron-irradiated CdS (see Appendix B). A long τ_0 does not necessarily imply that τ_n is correspondingly long. The comparison here does show, however, that for the observed τ_n the condition $\tau_0 \geq \tau_n$ is consistent with our observations and those of other experimenters.

Long lifetimes are associated with crystal imperfections (such as defects, impurities, and defect-impurity complexes). Some imperfections were present before irradiation and others were introduced as a result of the irradiation. Bube and Barton[34] performed photoconductivity experiments on LRC and have observed that some LRC are highly sensitive (i.e., have large $\mu\tau$ products). A general way of preparing photosensitive HRC has been to incorporate acceptors in the sensitive LRC (e.g., by annealing in a sulfur atmosphere). This is done in such a manner that the crystal

[34] R. H. Bube and L. A. Barton, RCA Rev. **20**, 564 (1959).

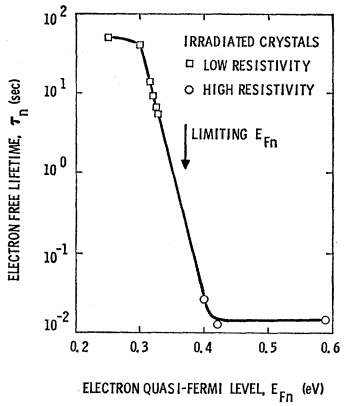

FIG. 5. Dependence of the electron free lifetime (τ_n) on the electron quasi-Fermi level (E_{Fn}) in fast-neutron-irradiated CdS. τ_n was determined from the induced conductivity resulting from radioactive decay. E_{Fn} is the position of the electron quasi-Fermi level below the edge of the conduction band at ~1 day following irradiation. Each datum point was obtained from a different sample. These results show that τ_n increases by a factor of $\sim 10^3$ when E_{Fn} decreases and shifts through the limiting position of E_{Fn}. These results were confirmed by γ-induced conductivity and photoconductivity experiments (Appendix B).

changes from the low-resistivity state to the high-resistivity state while retaining the photosensitivity. CdS is generally available in either the low-resistivity state ($<10^1$ Ω cm) or in the high-resistivity state ($>10^6$ Ω cm). It is difficult to obtain material with dark resistivities in the intermediate range by chemical doping because the degree of compensation is critical and is difficult to control. In these experiments material has been obtained in this range in a controlled manner by introducing defects with fast-neutron irradiation. These defects are probably responsible for the long lifetimes observed in these experiments.

Lifetime Mechanism

The dependence of τ_n on E_{Fn} is probably associated with the same mechanisms that are responsible for high sensitivity in photoconductors like CdS. Bube[30–32,34] has described these processes in detail. Before proceeding, consider the following: (1) Sensitizing centers are centers with large capture cross sections for holes but small capture cross sections for electrons. In sensitive photoconductors these centers are compensated acceptors and are probably intrinsic crystal defects or defect-impurity complexes. Many characteristics of photoconductors are directly related to the location of the energy levels of these centers. (2) A hole demarcation level E_{dp} is defined as that position in the forbidden gap where the probability of thermal exchange of a hole with the valence band equals the probability of recombination with a free electron from the conduction band. (Here E_{dp} is measured with respect to the valence band). Thus, the position of E_{dp} for a given sensitizing center determines whether that center acts as a trapping center (E_{dp} above center position)

or as a recombination center (E_{dp} below center position). (A recombination center is here defined as a center whose occupancy is defined by recombination kinetics.) High photosensitivity and thus large τ_n occur when sensitizing centers are recombination centers. The change in τ_n observed here can result from the conversion of a sensitizing center from a trapping center to a recombination center.

Let us now consider how such a change in kinetics can occur. Sensitizing centers can be associated with imperfections in the material before irradiation or introduced as a result of irradiation. For a particular state of the crystal some of these centers could be trapping centers (τ_n unaffected) or recombination centers (resulting in large τ_n). The position of E_{dp} for a particular sensitizing center depends on the electron concentration n. Thus, as n (or E_{Fn}) varies so does E_{dp}. A change in these parameters can result from changes in ionization, temperature, or doping. In these experiments such changes are associated with fast-neutron-induced defects and self-ionization effects. For irradiated samples where E_{Fn} is $\lesssim 0.37$ eV, τ_n is a factor of $\sim 10^3$ greater than that for irradiated samples where E_{Fn} is $\gtrsim 0.37$ eV. The results of these experiments suggest that for the case where E_{Fn} decreases and shifts across the limiting position of E_{Fn} there is a corresponding shift (decrease) in E_{dp} for a particular sensitizing center which converts that center from a trapping center to a recombination center. This would result in an increased τ_n. (Note that for the samples analyzed here changes in ionization with time after irradiation for a particular sample did not shift E_{Fn} through the limiting position of E_{Fn}. If it had, τ_n for that sample would have changed and such phenomena as superlinearity and quenching would have been observed in the induced-conductivity data.) The position of the sensitizing center responsible for the long lifetimes depends on the limiting position of E_{Fn}. Thus, this center probably results from the fast-neutron irradiation. Unfortunately, the position of this center could not be determined because the capture cross sections were unknown.

The long lifetimes observed here may be associated with fast-neutron-induced defect clusters. Work by Gregory[35] has shown that in Si the recombination kinetics of defect clusters are different than that of individual defects. It is very likely that in CdS the ratio of the capture cross section for holes to that for electrons is considerably greater for a defect cluster than for an individual intrinsic defect. The lifetimes associated with the fast-neutron-induced defect clusters would thus be longer than that associated with intrinsic crystal defects.

[35] B. L. Gregory, Bull. Am. Phys. Soc. 13, 464 (1968); also (private communication).

SUMMARY AND CONCLUSIONS

The effects of fast-neutron irradiation on the electrical properties of CdS have been determined. Both low- and high-resistivity single crystals were irradiated with 14-MeV neutrons (this study) and reactor-fast neutrons (previous study) to fluences ranging from 10^{10}–10^{17} neutrons/cm^2. Throughout this paper the effects of 14-MeV and reactor-neutron irradiations have been compared. The results have shown that in CdS the same kinds of defects are introduced by 14-MeV neutrons and reactor-fast neutrons. This was determined from the changes in resistivity with fluence, from the dependence of τ_n on E_{Fn}, and from the characteristics of thermal annealing. The results have further shown that the room-temperature annealing of neutron-induced defects is dependent upon the position of the electron quasi-Fermi level E_{Fn} below the edge of the conduction band.

In this study the changes in resistivity (or conductivity) with time after irradiation have been correlated with the measured decay of radioactivity from CdS. After accounting for annealing effects the results have shown that induced conductivity results from the β decay of ^{115}Cd (2.3-day half-life) and ^{32}P (14.3-day half-life). Ionization resulting from the absorption of the β radiation produces the induced conductivity. Absorption of γ radiation from the ^{115}Cd decay was insignificant. The electron free lifetime (τ_n) was determined from the induced conductivity, the mobility, the β decay rate, the radiation-ionization energy, and the average energy absorbed per β particle. The results from 14-MeV and reactor-neutron-irradiated CdS showed that τ_n was dependent on the resistivity, and therefore on E_{Fn}. When E_{Fn} is $\gtrsim 0.37$ eV ($\rho \gtrsim 2\times 10^4\ \Omega$ cm), τ_n is of the order of tens of msec. However, for $E_{Fn} \lesssim 0.37$ eV, the value of τ_n is larger by a factor of $\sim 10^3$. The value of $E_{Fn} \approx 0.37$ eV is the limiting position of E_{Fn} in fast-neutron-irradiated CdS (at ~ 1 day after irradiation), and depends on the induced defects as well as ionization. (The dependence of τ_n on E_{Fn} was confirmed by experiments on γ-induced conductivity and on photoconductivity in both neutron-irradiated and unirradiated CdS samples.) The large increase in τ_n with decreasing E_{Fn} probably results from changing the occupancy of sensitizing centers from being determined by thermal equilibrium kinetics to being determined by recombination kinetics. These centers probably result from fast-neutron irradiation and are associated with induced defects or defect clusters.

These experiments have yielded electron free lifetimes from induced conductivity in material with dark resistivities in the range which is not easily obtained by chemical doping (i.e., 10^1–$10^6\ \Omega$ cm). The unique features of these experiments were that the resistivity was obtained in this range by radiation doping and

that τ_n was determined from the self-ionization resulting from the β decay of radioisotopes.

Similar radioactive decay effects can probably be observed in other materials. Such effects would be most significant in high-resistivity materials that have large mobility-lifetime products. Many of the II–VI, III–V, and IV semiconductors possess these characteristics. Whether such effects will be detectable will also depend upon parameters such as the macroscopic-reaction cross section, the decay constant, and the amount of radiation energy absorbed.

ACKNOWLEDGMENTS

The authors gratefully acknowledge many helpful discussions with G. C. Smith and H. J. Stein, and the technical assistance of D. D. Drummond and D. J. Vanata.

APPENDIX A: RESISTIVITY INHOMOGENEITIES

Recent experiments by English and Parsons[36] using an electron-mirror microscope (EMM) have shown that high-resistivity CdS single crystals contain severe resistivity inhomogeneities. The EMM technique provides a means of mapping out regions of nonuniformity. Unfortunately, such instrumentation is not generally available to most experimenters for routine sample examination and other techniques must often be used to identify sample uniformity. In this study the 4-terminal van der Pauw technique[37] of measuring resistivities was used to provide this information. The purpose of this appendix is to outline this technique and to report on the results obtained from a random selection of crystals commercially available from three different suppliers.

The van der Pauw method of measuring electrical resistivities is a general technique applicable to thin arbitrary shaped samples with small electrical contacts arbitrarily positioned on the periphery, such as shown in Fig. 6(a). The development by van der Pauw assumes that the material is homogeneous. Transfer resistances are defined as follows:

$$R_{1234}=V_{34}/I_{12} \tag{10}$$

is the voltage drop across contacts 3 and 4 divided by the current flowing through contacts 1 and 2. There are eight different combinations, including reversals of polarity for current and voltage, which give the same value of transfer resistance. This generalized set is here defined as R_1. For resistivity measurements another set of transfer resistances is utilized, one of which is R_{2341}. This generalized set is similarly defined as R_2. The resistivity is given by

$$\rho=(\pi w/\ln 2)[(R_1+R_2)/2]f, \tag{11}$$

where w is the sample thickness and f is a geometric correction which is a function of the ratio R_1/R_2. For symmetric samples with symmetrically spaced contacts [such as shown in Fig. 6(b)] $R_1=R_2$ and $f=1$, thus $\rho=(\pi w/\ln 2)R_1$. If such symmetric samples, however, are found to have $R_1\neq R_2$, then it must be concluded that the samples do not have uniform electrical properties. Thus, the ratio R_1/R_2 can be used as an indication of the electrical uniformity of samples.[38] Note that $R_1/R_2=1$ is a necessary but not sufficient condition for homogeneity.

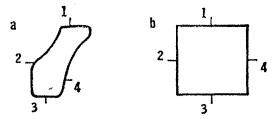

FIG. 6. Sample and contact arrangements when using the van der Pauw technique: (a) arbitrary geometry and (b) symmetrical geometry.

Resistivity measurements using the van der Pauw technique and sample geometry shown in Fig. 6(b) have been completed on both low- and high-resistivity CdS single crystals. The highly conducting LRC were generally uniform (i.e., $R_1/R_2\approx 1$), whereas the HRC were not. A total of 46 high-resistivity samples with dark resistivities ranging from 10^6–10^{10} Ω cm were examined. The results are given in Table IV and show that $R_1/R_2>2$ for over 50% of the samples in the dark-resistivity state. The range of values for the R_1/R_2 ratios given in Table IV are in good agreement with resistance ratios measured by Robertson and Ash[39] using optical probe techniques. In the present experiments it was found that almost all samples had $R_1/R_2\leq 2$ when in the photoconducting state (exposed to room light). This improved uniformity probably occurs because of a reduction of high-resistance barriers in the material.[30] It has also been generally observed that samples cut from the same initial crystal do not have the same initial resistivities, and thus it is not unusual to find nonuniformities in individual samples. There was no pronounced difference in samples obtained from different suppliers.

TABLE IV. Transfer resistance ratios[a] determined using the van der Pauw technique on geometrically symmetric high-resistivity CdS single crystals in the dark.

R_1/R_2	Number of samples
1–2	21
2–4	12
4–10	6
>10	7

[a] Electrical measurements and sample assymetries were such that ratios between 1 and 1.5 were considered to be within experimental error.

[36] F. L. English and M. K. Parsons, in *II–VI Semiconducting Compounds*, edited by D. G. Thomas (W. A. Benjamin, Inc., New York, 1967), p. 190; Appl. Phys. Letters **11**, 283 (1967).

[37] L. J. van der Pauw, Philips Res. Rept. **13**, 1 (1958); Philips Tech. Rev. **20**, 220 (1959).

[38] T. M. Baleshta and J. D. Keys, Am. J. Phys. **36**, 23 (1968).

[39] G. I. Robertson and E. A. Ash, Solid-State Electron. **11**, 603 (1968).

APPENDIX B: γ-INDUCED CONDUCTIVITY AND PHOTOCONDUCTIVITY

The dependence of τ_n on E_{Fn} (Fig. 5) was confirmed by independent experiments which examined the γ-induced conductivity and photoconductivity in a neutron-irradiated LRC (sample 1), a neutron-irradiated HRC (sample 2), and an HRC which was not exposed to neutron irradiation (sample 3). The characteristics of these samples both before and after neutron irradiation are given in Table V. The E_{Fn} for the unirradiated sample and for the irradiated samples after neutron exposure are given in Table V. Also given in this table are the expected values of τ_n for these samples as determined from the dependence of τ_n on E_{Fn}, which was determined from the results from the β-decay experiments (see Fig. 5, Table III, and the discussion in footnote d of Table V). The results of the analysis of induced conductivity from β decay predict that, for these samples, the ratio of the lifetimes of the neutron-irradiated LRC to that of the neutron-irradiated HRC is $\tau_1/\tau_2 \approx 67$. The corresponding ratio of the lifetime of the irradiated HRC to that of the unirradiated HRC is $\tau_2/\tau_3 \approx 1$. These results are summarized in Table VI.

An independent determination of these lifetime ratios for these three samples was obtained by exposing each sample to a constant γ-radiation intensity and to a constant optical-radiation intensity, and by measuring the corresponding induced conductivities. (Some of the details of these experiments are given as footnotes in Table VI.) For a constant excitation intensity the induced conductivity is proportional to the mobility-lifetime product [see Eq. (9)]. After accounting for sample-to-sample mobility differences the ratios of the electron free lifetimes in these samples were determined from the induced conductivity ratios. The results of these experiments are given in Table VI and show that the lifetime ratios measured from the γ-induced conductivity experiment and from the photoconductivity experiment are in good agreement with that predicted from the ^{32}P β-decay experiments. These results provide an independent "one-point" confirmation of the dependence of τ_n on E_{Fn} in neutron-irradiated CdS. It would of course be desirable to have a complete set of experiments in which τ_n was determined as E_{Fn} was varied (e.g., by varying the neutron fluence, γ-radiation intensity, optical-radiation intensity, or temperature). Lifetime ratios as high as 10^3 should be observed consistent with the dependence of τ_n on E_{Fn}, as shown in Fig. 5.

It is concluded that these experiments have confirmed (1) the observation of induced conductivity from β decay in neutron-irradiated CdS, (2) that lifetimes of the order of seconds are observed in neutron-irradiated LRC, (3) that the dependence of τ_n on E_{Fn} in neutron-irradiated CdS is given by Fig. 5, and (4) that the model of induced conductivity from β decay is correct.

TABLE V. Characteristics of samples used for verification of the dependence of the electron free lifetime τ_n on the electron quasi-Fermi level E_{Fn}.

Sample[a]	Dark resistivity (Ω cm)[b] Initial		After neutron irradiation	E_{Fn}[c] (eV)	τ_n[d] (sec)
1	6.9	(LRC)	1.2×10^4	0.35	1
2	2×10^{10}	(HRC)	1.4×10^6	0.47	15×10^{-3}
3	2×10^{10}	(HRC)	. . .	0.85	15×10^{-3}

[a] Samples 2 and 3 were cut from the same crystal.
[b] LRC and HRC denote low- and high-resistivity crystals. Samples 1 and 2 were irradiated to fast-neutron fluences of $\sim2\times10^{16}$ neutrons/cm^2 [$\sim2\times10^{15}$ neutrons/cm^2 (>3 MeV)]. The resistivites after irradiation were measured ~1 day following exposure.
[c] For samples 1 and 2, E_{Fn} is the position at ~1 day after neutron irradiation. Hall mobilities for samples 1, 2, and 3 were approximately 270, 230, and 280 cm^2/V sec, respectively.
[d] Expected values: Determined from Fig. 5 and Table III for the irradiated samples 1 and 2. The value for sample 3 should be approximately the same as for sample 2 as predicted by the model which was proposed to explain the dependence of τ_n on E_{Fn}, and in comparison with the photoconductivity experiments on unirradiated crystals by other investigators.

TABLE VI. Comparison of electron free lifetime ratios determined from (1) induced conductivity from β decay, (2) γ-induced conductivity, and (3) photoconductivity in two fast-neutron-irradiated CdS samples and one unirradiated CdS sample. τ_1, τ_2, and τ_3 are the lifetimes of an irradiated LRC (sample 1), and irradiated HRC (sample 2), and an unirradiated HRC (sample 3), respectively.[a]

Excitation source[b]		Lifetime ratios τ_1/τ_2	τ_2/τ_3
β-induced conductivity[c]	(predicted)	67	1
γ-induced conductivity[d]	(measured)	92	1.1
Photoconductivity[e]	(measured)	58	1.5

[a] Sample characteristics are given in Table V.
[b] The γ-induced conductivity and photoconductivity experiments were performed 30–40 days after neutron irradiation. This allowed time for the induced-β intensity to decrease significantly, whereas only a small percentage of the neutron-induced defects had thermally annealed. The intensities of the γ-radiation source and the optical-radiation source were chosen so that the induced conductivity was approximately the same as that obtained from the initial ^{32}P β decay in the irradiated samples. Response times to the rise and decay of γ-induced conductivity and photoconductivity varied from ~30 min in the unirradiated sample to several hours in the irradiated samples. The irradiated LRC had the longest response times.
[c] Predicted values as determined from the ^{32}P β-decay experimental results (see discussion in footnote d, Table V).
[d] ^{60}Co γ radiation; performed using Sandia Laboratories Vertical Gamma Range, Serial Number J204, ALO primary standard. γ dose rate was 50 rad/hr (note, the initial dose rate from ^{32}P β decay in a CdS crystal irradiated to $\sim2\times10^{16}$ neutrons/cm^2, >3 MeV, is ~50 rad/hr).
[e] Optical radiation filtered through a CdS crystal and a $CuSO_4$ solution in order to provide uniform excitation throughout the samples and to minimize optical quenching.